Global predictions of short- to medium-term COVID-19 transmission trends : a retrospective assessment

Sangeeta Bhatia (s.bhatia@imperial.ac.uk)
Imperial College London https://orcid.org/0000-0001-6525-101X

Kris Parag
Imperial College London https://orcid.org/0000-0002-7806-3605

Jack Wardle
Imperial College London

Natsuko Imai
Imperial College London https://orcid.org/0000-0002-4218-9716

Sabine van Elsland
Imperial College London

Britta Lassmann
International Society for Infectious Diseases

Gina Cuomo-Dannenburg
Imperial College London https://orcid.org/0000-0001-6821-0352

Elita Jauneikaite
Imperial College London https://orcid.org/0000-0002-7075-6896

H. Juliette Unwin
Imperial College London https://orcid.org/0000-0002-9120-4003

Steven Riley
Imperial College

Neil Ferguson
Imperial College London https://orcid.org/0000-0002-1154-8093

Christl Donnelly
Imperial College London https://orcid.org/0000-0002-0195-2463

Anne Cori
Imperial College - Faculty of Medicine

Pierre Nouvellet
University of Sussex https://orcid.org/0000-0002-6094-5722

Article

Keywords: COVID-19, SARS-CoV-2, transmission, public health

Posted Date: August 13th, 2021

DOI: https://doi.org/10.21203/rs.3.rs-799162/v1

Global predictions of short- to medium-term COVID-19 transmission trends : a retrospective assessment

Sangeeta Bhatia[1, *], Kris V Parag[1], Jack Wardle[1], Natsuko Imai[1], Sabine L Van Elsland[1], Britta Lassmann[2], Gina Cuomo-Dannenburg[1], Elita Jauneikaite[1], H. Juliette T. Unwin[1], Steven Riley[1], Neil Ferguson[1], Christl A Donnelly[1, 3], Anne Cori[1], Pierre Nouvellet[1, 4]

1 MRC Centre for Global Infectious Disease Analysis, School of Public Health, Imperial College London, UK.

2 ProMED, International Society for Infectious Diseases, Brookline, MA, USA.

3 Department of Statistics, University of Oxford, Oxford, UK.

4 School of Life Sciences, University of Sussex, Brighton, UK.

* s.bhatia@imperial.ac.uk

Abstract

From 8th March to 29th November 2020, we produced weekly estimates of SARS-CoV-2 transmissibility and forecasts of deaths due to COVID-19 for 81 countries with evidence of sustained transmission. We also developed a novel heuristic to combine weekly estimates of transmissibility to produce forecasts over a 4-week horizon. We evaluated the robustness of the forecasts using relative error, coverage probability, and comparisons with null models. During the 39-week period covered by this study, both the short- and medium-term forecasts captured well the epidemic trajectory across different waves of COVID-19 infections with small relative errors over the forecast horizon. The model was well calibrated with 56.3% and 45.6% of the observations lying in the 50% Credible Interval in 1-week and 4-week ahead forecasts respectively. We could accurately characterise the overall phase of the epidemic up to 4-weeks ahead in 84.9% of country-days. The medium-term forecasts can be used in conjunction with

the short-term forecasts of COVID-19 mortality as a useful planning tool as countries continue to relax public health measures.

Introduction

As of July 2021, more than 4 million deaths have been attributed to COVID-19 with over 180 million cases reported globally [1]. The scale of the current pandemic has led to a widespread adoption of data-driven public health responses across the globe. Outbreak analysis and real-time modelling, including short-term forecasts of future incidence, have been used to inform decision making and response efforts in several past public health challenges including the West African Ebola epidemic and seasonal influenza [2–11]. In the current pandemic, mathematical models have helped public health officials better understand the evolving epidemiology of SARS–CoV-2 [12–14] and the potential impact of implementing or releasing interventions. Short-term forecasts of key indicators such as mortality, hospitalisation, and hospital occupancy have played a similarly important role [15–20], contributing to planning public health interventions and allocation of crucial resources [21–25]. At the same time, the unprecedented level of public interest has placed epidemiological modelling under intense media scrutiny. In light of the prominent role mathematical models have had in policy planning during the COVID-19 pandemic, retrospective assessment of modelling outputs against later empirical data is critical to assess their validity.

With the aim of improving situational awareness during the ongoing pandemic, since the 8th March 2020 we have been reporting weekly estimates of transmissibility of SARS–CoV-2 and forecasts of the daily incidence of deaths associated with COVID-19 for countries with evidence of sustained transmission [26]. We have developed three models that are calibrated using the latest reported incidence of COVID-19 cases and deaths in each country. We combined the outputs from the the three models into an ensemble and estimates of transmissibility and forecasts were based on the ensemble model. Ensemble models, which combine outputs from different models, are a powerful way of incorporating the uncertainty from a range of models [27, 28] and can produce more robust forecasts than individual models [28–31].

Forecasts are typically produced under the assumption that the trend in growth

remain the same over the forecast horizon. This is a plausible assumption for the 1-week forecast horizon that we used for our short-term forecasts. However, this assumption is likely to be violated over a long forecast horizon leading to a rapidly increasing uncertainty as the forecast horizon grows. We have developed a novel approach relying on a simple heuristic that combines past estimates of the reproduction number, explicitly accounting for the predicted future changes in population immunity, to produce forecasts over longer time horizons.

Here we summarise the key transmission trends from our work on global short-term forecasts between 8th March to 29th November 2020. We provide a rigorous quantitative assessment of the performance of the ensemble model. We also present medium-term forecasts using our approach and retrospectively assess the performance of our method. Our results for medium-term forecasts suggest that we can accurately forecast the trajectory of COVID-19 in several countries for horizons spanning up to 4 weeks.

Results

Methods for estimating transmissibility during epidemics typically rely on the time series of incident cases combined with the natural history parameters of the pathogen [32, 33]. However, in the current pandemic, interpretation and comparison of estimates across countries based on the number of cases was made difficult by the differences in case definitions, testing regimes, and variable reporting across countries as well as over time within each country [34]. We therefore developed three different models that relied on the number of reported deaths to estimate COVID-19 transmissibility and to produce short- and medium-term ensemble forecasts of deaths (1- and 4- week ahead respectively). The methods underlying the individual models are illustrated in Figs. 1a to 1c (see Methods and SI Sec. 2 for details).

Beginning 8th March 2020, we produced weekly forecasts for every country with evidence of sustained transmission. As the pandemic rapidly spread across the world, the number of countries included in the weekly analysis grew from 3 in the first week (week beginning 8th March 2020), to 94 in the last week of analysis included in this study (week beginning 29th November 2020) (SI2 Fig. 1). Our results are based on the analysis done for 81 countries (see SI Sec. 5 for exclusion criterion) over the 39 week

period from 8th March to 29th November 2020 .

Short-term forecasts and model performance

Overall, the ensemble model performed well in capturing the short-term trajectory of the epidemic in each country. Across all weeks of forecast and all countries, an average 58.7% (SD 32.4%) of the observations were in the 50% credible interval (CrI) and 89.4% (SD 21.7%) of the observations were in 95% CrI (for a breakdown by country and week of forecast see SI2 Sec. 2.5).

The MRE across all countries and all weeks was 0.4 (SD 0.4) (Fig. 3). That is, on average the model forecasts were 0.4 times lower or higher than the observed incidence. In most countries, the reporting of both cases and deaths through the week was variable, with fewer numbers reported on some days of the week (typically, Saturday and Sunday). The variability in reported deaths strongly influenced the model performance. The MRE scaled linearly with the coefficient of variation (ratio of the standard deviation to the mean) in the reported deaths for the week of forecasting. Thus, the error in forecasts was on average similar to the variability in the reported deaths (SI2 Fig. 3). The MRE of the model scaled inversely with the weekly incidence i.e. the error was relatively large when the incidence was low (SI2 Fig. 3), as estimates of reproduction number when the incidence is low are inherently more unstable [35].

The model performance was largely consistent across epidemic phases (growing, likely growing, decreasing, likely decreasing and indeterminate (SI Sec. 4)) with similar coverage probability and MRE (SI2 Table 1). The slightly larger proportion of observations in the 50% and 95% credible intervals for the 'indeterminate' phase and the larger MRE in this phase together suggest that the model was 'under-confident' with large credible intervals [36].

We compared the performance of the model with that of a null no-growth model. In most instances, the ensemble model outperformed the null model. In 80.9% of the weeks in 'definitely decreasing' phase and 61.4% of weeks in 'definitely growing' phase, the absolute error of the model was smaller than the error made by the null model (Fig. 3, SI2 Sec. 2.2, SI2 Table 2). The null model performed better when the trajectory of the epidemic in a country was relatively stable exhibiting little to no change over the time

frame of comparison. This is to be expected as the null model describes precisely this stable dynamic. Indeed, in 68.1% of the weeks in the 'likely growing' phase and 67.1% weeks classified as 'indeterminate' phase, the absolute error of the model was larger than the error made by the null model. However, the relative error of the model remained small even in countries and weeks where it did not perform as well as the null model. Similarly, our model performed better than a linear growth model across all phases, specifically in 96.4% of the weeks in 'definitely decreasing' phase and 70.3% weeks in 'definitely growing' phase (SI2 Sec. 2.3, SI2 Table 2).

Medium-term forecasts and model performance

The rapidly changing situation and the various interventions deployed to stem the growth of the pandemic make forecasting at any but the shortest of time horizons extremely challenging [37]. Despite these challenges, we find that our medium-term forecasts were able to robustly capture the epidemic trajectory (Fig. 4) in all countries included in the analysis (4).

Overall, the MRE remained small over a 4-week forecast horizon, with errors increasing over the projection horizon (SI2 Sec. 3.1). We therefore restricted the projection horizon to 4 weeks. The MRE across all countries in 1-week ahead forecasts was 0.4 (SD 0.3), increasing to 2.6 (SD 28.3) in 4-week ahead forecasts (Fig. 5, SI2 Fig. 7). The MRE for 1-week ahead forecasts was less than 1 (indicating that the magnitude of the error was smaller than the observation) in 91.1% of weeks for which we produced forecasts. The corresponding figure for 4-week ahead forecasts was 66.0% (SI2 Table 3).

The proportion of observations in the 50% CrI remained consistent across the forecast horizon and varied from 56.3% (SD 33.4%) in 1-week ahead forecasts to 45.6% (SD 40.9%) in 4-week ahead forecasts (SI2 Fig. 8, SI2 Fig. 9).

Across the 81 countries and 2210 weeks (15470 days) for which we produced both short- and medium-term forecasts, the phase definition using the reproduction number estimates from medium-term forecasts, R_t^S (SI Sec. 3 and SI Eq. 11), was consistent with that using the estimates from the short-term forecasts (R_t^{curr}) in 87.6% (13559/15470) of country-days (number of countries X number of days for which we produced forecasts. The phase definition using reproduction number estimates from medium-term forecasts

was updated each day over the forecast horizon while the short-term forecasts assigned the same phase to all days of a week.) in 1-week ahead forecasts and in 84.9% (13138/15470) of country-days in 4-week ahead forecasts (Fig. 6). When the phase definitions using R_t^S and R_t^{curr} were different, the medium-term estimates most frequently misclassified them as a phase with greater uncertainty. For instance, in 253 weeks when the epidemic phase was identified as 'definitely decreasing' using weekly estimates and incorrectly characterised using medium-term estimates, it was misclassified as 'likely decreasing' in 100% (253/253 weeks) of country-days. Similarly, in the misclassified weeks, when the epidemic phase using weekly transmissibility estimates was 'definitely growing', the medium-term classification was 'indeterminate' in 43.7% (1175/2688) and 'likely growing' in 56.3% (1513/2688) of the country-days. This mis-characterisation is expected as the uncertainty in estimates of R_t^S grows over the forecast horizon. Crucially, none of the weeks where R_t^S misclassified the epidemic phase, the phase using R_t^{curr} indicated the opposite trend (growing classified as decreasing or vice versa). This finding shows that the medium-term transmissibility estimates can be used a reliable indicator of the overall direction of the epidemic trajectory.

Discussion

Models used to forecast COVID-19 cases and/or deaths vary in complexity in the data used for model calibration. More complex and/or granular models rely on multiple data streams including data on hospital admissions and occupancy, testing, serological surveys and data on patient clinical progression and outcomes [21]. Such complex location-specific models can provide crucial insights into the ongoing epidemic and inform targeted public health interventions by synthesising evidence from different data streams. However, scaling such analysis to include multiple geographies is challenging because of the variability in availability and reliability of local surveillance data. The computational time needed to fit complex models make scaling them difficult and delays the timely provision of risk estimates.

In addition to the variable availability of surveillance data across countries, the wide-scale societal and behavioural changes brought about by the pandemic impose practical constraints on utilising data that are available for multiple countries. For instance, widely

available data on the changes in mobility inferred from mobile phone usage released by Google and Apple were informative of the changes in transmission in the early phase of the COVID-19 pandemic and were used in several modelling studies [38, 39]. Although these data continue to be available, recent evidence suggests a decoupling of transmission and mobility in most countries [40, 41]. Models that relied on such additional data [39] or assumptions about non-pharmaceutical interventions [42] could not fit the observed trajectory well as the situation continued to change over the course of the epidemic.

Efforts to model and forecast COVID-19 transmission dynamics must therefore meet the challenges of a long and ongoing pandemic spread over an unprecedented scale. Modelling groups around the world have attempted to meet one or both challenges with various analyses conducted at a sub-national scale [43], at a national scale for a specific country [22, 44–46], and for several countries across the globe [47–49]. In contrast to models built for a region or country and calibrated using local data, models that aim to provide a global overview must be sufficiently general to describe the epidemic trajectory in a range of countries/regions using widely available data that are consistently available over time.

We have produced short-term forecasts and estimates of transmissibility for 81 countries for more than 65 weeks at the time of writing implementing three simple models that use only the time series of COVID-19 cases and deaths. We have thus traded particularity for generality, to allow us to carry out analysis for a large number of countries over a long period of time. As our methods make few assumptions and use routine surveillance data, they can be easily used during any other future outbreaks.

Despite the challenges inherent in forecasting a fast-moving pandemic in the presence of unprecedented public health interventions, our ensemble model was able to successfully capture the short-term transmission dynamics across all countries included in the analysis with small relative error in the weekly forecasts across different COVID-19 waves in each country. The variable performance of our model in weeks and countries with fewer deaths and/or large variability in reported deaths over weeks reflects this trade-off. In the absence of more detailed data, we assumed that epidemiological parameters such as the delay from onset of symptoms to death were the same across all countries and throughout the period of analysis. These parameters are likely to vary over time and between countries and using country-specific parameters could lead to moderate

improvements in the model fits and forecast performance.

Due to the variability in testing and reporting of cases across different countries and over time within countries, using the reported number of cases to estimate transmissibility and produce forecasts is difficult without using more complex models. For these reasons, we primarily used deaths to estimate the reproduction number as we assumed that reporting of COVID-19 deaths was more complete and consistent over time and across different country surveillance systems. Although this assumption is unlikely to hold for many countries [50–52], our methods are robust to a constant rate of under-reporting over time as this would not alter the overall epidemic trends. A limitation of our work is that our estimates reflect the epidemiological situation with a delay of approximately 19 days (the delay from an infection to a death [42]). Nevertheless, our short-term forecasts and transmissibility estimates provide a valuable global overview and continuous insights into the dynamic trajectory of the epidemic in different countries. They also provide indirect evidence about the effectiveness of public health measures. Future research could investigate integrating more data streams into the models. In addition to the weekly reports that we publish, our work has also contributed to other international forecasting efforts [22, 36, 44].

We developed a simple heuristic to combine past estimates of transmissibility and a decline in the proportion of susceptible population to produce medium-term forecasts. We were able to achieve good model performance in forecasting up to 4 weeks ahead. Consistent with findings from other modelling studies [22], we found that the model error was unacceptably high beyond 4 weeks, suggesting that forecasting beyond this horizon is difficult. Importantly, our characterisation of the epidemic phase using weighted estimates of transmissibility were largely in agreement with that using short-term transmissibility estimates. Thus, our method was successful at capturing the broad trends in transmission up to 4 weeks ahead. The medium-term forecasts can therefore serve as a useful planning tool as governments around the world plan further implementation or relaxation of non-pharmaceutical interventions.

Our method incorporates the depletion of susceptible population and hence can in principle be extended to account for increasing population immunity as vaccination is rolled out across the world. However, inclusion of vaccine induced immunity depends on the availability of reliable data on vaccination coverage. Further, even if such data

were available, teasing apart the impact of vaccination on transmission and mortality could be non-trivial. In light of these issues, it might be challenging to extend our approach to rigorously assess the effect of vaccination on epidemic trajectory on a global scale. However, our latest estimates of transmissibility indirectly reflect the impact of vaccination on transmission, allowing for the delay from vaccination to full immunity, and from infection to death. As we continue to track COVID-19 transmissibility globally, any temporal changes in transmissibility would implicitly account for the changes due to differential vaccination coverage.

Mathematical modelling and forecasting efforts have supported data-driven decision making throughout this public health crisis. Our work has aimed to improve global situational awareness. Using relatively simple approaches, we were able to produce robust forecasts for COVID-19 in 81 countries and provide crucial and actionable insights. This effort is being continued [26] as the world continues to grapple with renewed waves of COVID-19 cases.

Methods

The instantaneous reproduction number is frequently used to quantify transmissibility. It is defined as the average number of secondary cases that an individual infected at time t would generate if conditions remained as they were at time t [53]. When applied to the incidence of deaths (rather than cases), the instantaneous reproduction number R_t^D represents the average number of secondary deaths "generated by" the death of a primary case at time t. We developed three different models, each of which estimated transmissibility in the recent past and produced forecasts of COVID-19 deaths (SI Sec. 2.1 to 2.3). We then combined the outputs of these models to build an unweighted ensemble (SI Sec. 2.4). We produced short-term forecasts (i.e. 1-week ahead), for which changes in the population immunity level could be ignored. Over the course of the epidemic, the effect of the potential depletion of the susceptible population on the trajectory of the epidemic may become more pronounced. Inherently, by estimating transmissibility in real-time, our models account for any general decrease in the proportion of population being susceptible. However, the forecasts produced do not account for any further decrease in this proportion, which may become substantial when forecasting over a

medium- to long-term time horizon.

We also produced medium-term forecasts (up to 4-weeks ahead) accounting for the depletion of the susceptible population due to the increased levels of natural host immunity. In order to estimate transmissibility for medium-term forecasts, we combined past estimates of transmissibility into a single weighted estimate as follows. Let T denote the last time point in the existing incidence time series of cases or deaths and let R_T^{curr} refer to the the most recent estimate of reproduction number for a given model. Starting with the transmissibility estimates of R_T^{curr} from the ensemble model, we went back one week at a time, for as long as the 95% credible interval (CrI) of $R_{T'}^{curr}$ (where $T' < T$) overlapped the 95% CrI of R_T^{curr}. We then sampled from the posterior distribution of $R_{T'}^{curr}$ in each of those weeks, with a probability that decays exponentially in the past to favour the more recent estimates (Fig. 1d). Each week, the rate of decay β was optimised by minimising the relative error in the predictions for the previous week. As the weighted reproduction number R_t^w already accounts for the population immunity at time t, we first estimated an effective reproduction number defined as the reproduction number if the entire population were susceptible (SI Eq. 10). We then estimated the reproduction number R_t^S accounting for the effect of population immunity at time t due to infection (SI Eq. 11).

Forecast horizon

The short-term forecast horizon was set to be 1 week. We produced forecasts for the week ahead (Monday to Sunday) using the latest data up to (and including) Sunday. We did not model the potential changes in the population immunity levels as any such change is not expected to affect the trajectory of the epidemic over this short time horizon.

The medium-term forecasts were made over a 4-week horizon using R_t^S. Since estimates of the weighted reproduction number could only be obtained once we had sufficient weekly estimates to combine, medium-term forecasts were produced from 29th March to 29th November 2020.

Epidemic Phase

Following Abbott et al. [47], we defined the epidemic phase in a country at time t as 'likely growing', 'definitely growing', 'likely decreasing', 'definitely decreasing' or 'indeterminate' using the distribution of the reproduction number at t (R_t^{curr} for the short-term forecasts and R_t^S for the medium-term forecasts, SI Sec. 4).

Assessing model performance

The model forecasts were validated against observed deaths as these became available. To quantitatively assess the performance of the model for both short- and medium-term forecasts, we used the mean relative error (MRE) and the coverage probability i.e. the proportion of observations that are in a given credible interval of the distribution of forecasts (SI2 Sec. 2). We compared the absolute error of the model (the absolute difference between the forecasts and observations averaged across simulated trajectories) with the error of a model that used (i) the average of the last 10 observations as a forecast for the week ahead (no growth) [54], and (ii) forecasted using a linear model fitted to the last 10 observations (linear growth).

Data

We used the number of COVID-19 cases and deaths reported by the World Health Organisation (WHO) [1]. Any data anomalies were corrected using data published by the European Centre for Disease Prevention and Control [55], or other sources. All data used in the study are available at the github repository associated with this article (`https://github.com/mrc-ide/covid19-forecasts-orderly`).

Code

All analysis was carried out in R version 4.0.2. The code for the analysis is available as orderly [56] project at `https://github.com/mrc-ide/covid19-forecasts-orderly`. DeCa model is available as an R package at `https://github.com/sangeetabhatia03/ascertainr`. The accompanying R package `https://github.com/mrc-ide/rincewind` contains utility functions for creating the figures and processing model outputs.

Supporting information

S1 1. Supplementary Methods. The supplementary file contains a description of the methods and details on data, epidemiological parameters, and code.

S1 2. Supplementary Results. The supplementary file contains additional results on model performance.

S1 3. Web tool. An interactive web-tool available at `https://shiny.dide.imperial.ac.uk/covid19-forecasts-shiny/` presents both short- and medium-term forecasts, and reproduction number estimates for all countries included in the analysis.

Acknowledgements

The authors acknowledge funding from the MRC Centre for Global Infectious Disease Analysis (reference MR/R015600/1), jointly funded by the UK Medical Research Council (MRC) and the UK Foreign, Commonwealth & Development Office (FCDO), under the MRC/FCDO Concordat agreement and is also part of the EDCTP2 programme supported by the European Union. JW acknowledges research funding from the Wellcome Trust (grant 102169/Z/13/Z). SB acknowledges funding from the Wellcome Trust (219415). This study is partially funded by the National Institute for Health Research (NIHR) Health Protection Research Unit in Modelling and Health Economics, a partnership between Public Health England, Imperial College London and LSHTM (grant code NIHR200908); and acknowledges funding from the MRC Centre for Global Infectious Disease Analysis (reference MR/R015600/1), jointly funded by the UK Medical Research Council (MRC) and the UK Foreign, Commonwealth & Development Office (FCDO), under the MRC/FCDO Concordat agreement and is also part of the EDCTP2 programme supported by the European Union. The views expressed are those of the author(s) and not necessarily those of the NIHR, Public Health England or the Department of Health and Social Care.

Contributions

S.B. developed and implemented the methods and led the analysis. K.V.P. and J.W. contributed to development of code. P.N. designed the study, developed the methods and supervised the study. C.A.D and A.C. supervised the study and helped with revising the manuscript. All authors contributed to writing the manuscript.

References

1. WHO Coronavirus Disease (COVID-19) Dashboard; 2021. `https://covid19.who.int`.

2. Lipsitch M, Finelli L, Heffernan RT, Leung GM, Redd; for the 2009 H1N1 Surveillance Group SC. Improving the evidence base for decision making during a pandemic: the example of 2009 influenza A/H1N1. Biosecurity and Bioterrorism: Biodefense Strategy, Practice, and Science. 2011;9(2):89–115.

3. WHO Ebola Response Team. Ebola Virus Disease in West Africa – The First 9 Months of the Epidemic and Forward Projections. New England Journal of Medicine. 2014;371:1481–1495. doi:10.1056/NEJMoa1411100.

4. The Ebola Outbreak Epidemiology Team. Outbreak of Ebola virus disease in the Democratic Republic of the Congo, April & May, 2018: an epidemiological study. The Lancet. 2018;392:213–221. doi:10.1016/S0140-6736(18)31387-4.

5. Nsoesie E, Mararthe M, Brownstein J. Forecasting Peaks of Seasonal Influenza Epidemics. PLoS Currents. 2013;5. doi:10.1371/currents.outbreaks.bb1e879a23137022ea79a8c508b030bc.

6. Bogoch II, Brady OJ, Kraemer MU, German M, Creatore MI, Kulkarni MA, et al. Anticipating the international spread of Zika virus from Brazil. The Lancet. 2016;387(10016):335–336.

7. WHO Ebola Response Team. West African Ebola Epidemic after One Year — Slowing but Not Yet under Control. New England Journal of Medicine. 2015;372(6):584–587. doi:10.1056/NEJMc1414992.

8. Meltzer MI, Atkins CY, Santibanez S, Knust B, Petersen BW, Ervin ED, et al. Estimating the future number of cases in the Ebola epidemic–Liberia and Sierra Leone, 2014–2015. 2014;.

9. Barry A, Ahuka-Mundeke S, Ali Ahmed Y, Allarangar Y, Anoko J, Archer BN, et al. Outbreak of Ebola virus disease in the Democratic Republic of the Congo, April–May, 2018: an epidemiological study. The Lancet. 2018;392(10143):213–221. doi:10.1016/S0140-6736(18)31387-4.

10. Biggerstaff M, Johansson M, Alper D, Brooks LC, Chakraborty P, Farrow DC, et al. Results from the second year of a collaborative effort to forecast influenza seasons in the United States. Epidemics. 2018;24:26–33. doi:10.1016/j.epidem.2018.02.003.

11. for the Influenza Forecasting Contest Working Group, Biggerstaff M, Alper D, Dredze M, Fox S, Fung ICH, et al. Results from the Centers for Disease Control and Prevention's predict the 2013–2014 Influenza Season Challenge. BMC Infectious Diseases. 2016;16(1):357. doi:10.1186/s12879-016-1669-x.

12. Verity R, Okell L, Dorigatti I, Winskill P, Whittaker C, Imai N, et al. Estimates of the severity of coronavirus disease 2019: a model-based analysis. Lancet Infectious Diseases. 2020;doi:10.1016/S1473-3099(20)30243-7.

13. Nishiura H, Linton NM, Akhmetzhanov AR. Serial interval of novel coronavirus (COVID-19) infections. International Journal of Infectious Diseases. 2020;doi:10.1016/j.ijid.2020.02.060.

14. Ali ST, Wang L, Lau EH, Xu XK, Du Z, Wu Y, et al. Serial interval of SARS-CoV-2 was shortened over time by nonpharmaceutical interventions. Science. 2020;369(6507):1106–1109. doi:10.1126/science.abc9004.

15. Massonnaud C, Roux J, Crépey P. COVID-19: Forecasting short term hospital needs in France. medRxiv. 2020; p. 2020.03.16.20036939. doi:10.1101/2020.03.16.20036939.

16. Ahmadi A, Fadaei Y, Shirani M, Rahmani F. Modeling and forecasting trend of COVID-19 epidemic in Iran until May 13, 2020. Medical Journal of the Islamic Republic of Iran. 2020;34:27. doi:10.34171/mjiri.34.27.

17. Ferstad JO, Gu A, Lee RY, Thapa I, Shin AY, Salomon JA, et al. A model to forecast regional demand for COVID-19 related hospital beds. medRxiv. 2020; p. 2020.03.26.20044842. doi:10.1101/2020.03.26.20044842.

18. Reno C, Lenzi J, Navarra A, Barelli E, Gori D, Lanza A, et al. Forecasting COVID-19-Associated Hospitalizations under Different Levels of Social Distancing in Lombardy and Emilia-Romagna, Northern Italy: Results from an Extended SEIR Compartmental Model. Journal of Clinical Medicine. 2020;9(5):1492. doi:10.3390/jcm9051492.

19. IHME COVID-19 health service utilization forecasting team and Murray, Christopher JL. Forecasting COVID-19 impact on hospital bed-days, ICU-days, ventilator-days and deaths by US state in the next 4 months. medRxiv. 2020; p. 2020.03.27.20043752. doi:10.1101/2020.03.27.20043752.

20. Goic M, Bozanic-Leal MS, Badal M, Basso LJ. COVID-19: Short-term forecast of ICU beds in times of crisis. PLOS One. 2021;16(1):e0245272. doi:10.1371/journal.pone.0245272.

21. Knock ES, Whittles LK, Lees JA, Perez-Guzman PN, Verity R, FitzJohn RG, et al. Key epidemiological drivers and impact of interventions in the 2020 SARS-CoV-2 epidemic in England. Science Translational Medicine. 2021; p. eabg4262. doi:10.1126/scitranslmed.abg4262.

22. Ray EL, Wattanachit N, Niemi J, Kanji AH, House K, Cramer EY, et al. Ensemble Forecasts of Coronavirus Disease 2019 (COVID-19) in the U.S. medRXiv. 2020;doi:10.1101/2020.08.19.20177493.

23. Roosa K, Lee Y, Luo R, Kirpich A, Rothenberg R, Hyman J, et al. Real-time forecasts of the COVID-19 epidemic in China from February 5th to February 24th, 2020. Infectious Disease Modelling. 2020;5:256–263. doi:10.1016/j.idm.2020.02.002.

24. IHME COVID-19 Forecasting Team. Modeling COVID-19 scenarios for the United States. Nature Medicine. 2020;doi:10.1038/s41591-020-1132-9.

25. Chintalapudi N, Battineni G, Amenta F. COVID-19 disease outbreak forecasting of registered and recovered cases after sixty day lockdown in Italy: A data

driven model approach. Journal of Microbiology, Immunology and Infection. 2020;doi:10.1016/j.jmii.2020.04.004.

26. Short-term forecasts of COVID-19 deaths in multiple countries; 2021. https://mrc-ide.github.io/covid19-short-term-forecasts/.

27. Dormann CF, Calabrese JM, Guillera-Arroita G, Matechou E, Bahn V, Barton K, et al. Model averaging in ecology: a review of Bayesian, information-theoretic, and tactical approaches for predictive inference. Ecological Monographs. 2018;88(4):485–504. doi:10.1002/ecm.1309.

28. Buckee CO, Johansson MA. Individual model forecasts can be misleading, but together they are useful. European Journal of Epidemiology. 2020;35(8):731–732.

29. Johansson MA, Apfeldorf KM, Dobson S, Devita J, Buczak AL, Baugher B, et al. An open challenge to advance probabilistic forecasting for dengue epidemics. Proceedings of the National Academy of Sciences. 2019;116(48):24268–24274. doi:10.1073/pnas.1909865116.

30. Reich NG, McGowan CJ, Yamana TK, Tushar A, Ray EL, Osthus D, et al. Accuracy of real-time multi-model ensemble forecasts for seasonal influenza in the US. PLoS Computational Biology. 2019;15(11):e1007486. doi:10.1371/journal.pcbi.1007486.

31. Viboud C, Sun K, Gaffey R, Ajelli M, Fumanelli L, Merler S, et al. The RAPIDD Ebola forecasting challenge: Synthesis and lessons learnt. Epidemics. 2018;22:13–21. doi:10.1016/j.epidem.2017.08.002.

32. Wallinga J, Teunis P. Different epidemic curves for severe acute respiratory syndrome reveal similar impacts of control measures. American Journal of Epidemiology. 2004;160(6):509–516.

33. Cori A, Ferguson NM, Fraser C, Cauchemez S. A new framework and software to estimate time-varying reproduction numbers during epidemics. American Journal of Epidemiology. 2013;178(9):1505–1512. doi:10.1093/aje/kwt133.

34. Pullano G, Di Domenico L, Sabbatini CE, Valdano E, Turbelin C, Debin M, et al. Underdetection of cases of COVID-19 in France threatens epidemic control. Nature. 2021;590(7844):134–139. doi:10.1038/s41586-020-03095-6.

35. Parag KV. Improved estimation of time-varying reproduction numbers at low case incidence and between epidemic waves. Epidemiology; 2020. Available from: `http://medrxiv.org/lookup/doi/10.1101/2020.09.14.20194589`.

36. European Covid-19 Forecast Hub: Weekly reports; 2021. `https://covid19forecasthub.eu/reports`.

37. Castro M, Ares S, Cuesta JA, Manrubia S. The turning point and end of an expanding epidemic cannot be precisely forecast. Proceedings of the National Academy of Sciences. 2020;117(42):26190–26196. doi:10.1073/pnas.2007868117.

38. Vollmer MAC, Mishra S, Unwin HJT, Gandy A, Mellan TA, Bradley V, et al. A sub-national analysis of the rate of transmission of COVID-19 in Italy. Public and Global Health; 2020. Available from: `http://medrxiv.org/lookup/doi/10.1101/2020.05.05.20089359`.

39. Unwin HJT, Mishra S, Bradley VC, Gandy A, Mellan TA, Coupland H, et al. State-level tracking of COVID-19 in the United States. Nature Communications. 2020;11(1):1–9.

40. Nouvellet P, Bhatia S, Cori A, Ainslie KEC, Baguelin M, Bhatt S, et al. Reduction in mobility and COVID-19 transmission. Nature Communications. 2021;12(1):1090. doi:10.1038/s41467-021-21358-2.

41. Ainslie KEC, Walters CE, Fu H, Bhatia S, Wang H, Xi X, et al. Evidence of initial success for China exiting COVID-19 social distancing policy after achieving containment. Wellcome Open Research. 2020;5:81. doi:10.12688/wellcomeopenres.15843.2.

42. Flaxman S, Mishra S, Gandy A, Unwin HJT, Mellan TA, Coupland H, et al. Estimating the effects of non-pharmaceutical interventions on COVID-19 in Europe. Nature. 2020;584(7820):257–261. doi:10.1038/s41586-020-2405-7.

43. Mishra S, Scott J, Zhu H, Ferguson NM, Bhatt S, Flaxman S, et al. A COVID-19 Model for Local Authorities of the United Kingdom. medRxiv. 2020;.

44. Bracher J, Wolffram D, Deuschel J, Goergen K, Ketterer JL, Ullrich A, et al. Short-term forecasting of COVID-19 in Germany and Poland during the second wave–a preregistered study. medRxiv. 2020;doi:10.1101/2020.12.24.20248826.

45. COVID-19 Austria; 2021. https://www.covid19model.at.

46. Hawryluk I, Mellan TA, Hoeltgebaum H, Mishra S, Schnekenberg RP, Whittaker C, et al. Inference of COVID-19 epidemiological distributions from Brazilian hospital data. Journal of the Royal Society Interface. 2020;17(172):20200596.

47. Abbott S, Hellewell J, Thompson RN, Sherratt K, Gibbs HP, Bosse NI, et al. Estimating the time-varying reproduction number of SARS-CoV-2 using national and subnational case counts. Wellcome Open Research. 2020;5(112):112.

48. COVID-19 LMIC Reports; 2020. https://mrc-ide.github.io/global-lmic-reports/.

49. COVID-19 Daily Epidemic Forecasting; 2021. https://renkulab.shinyapps.io/COVID-19-Epidemic-Forecasting.

50. Alves THE, de Souza TA, de Almeida Silva S, Ramos NA, de Oliveira SV. Underreporting of death by COVID-19 in Brazil's second most populous state. Frontiers in Public Health. 2020;8.

51. Angulo FJ, Finelli L, Swerdlow DL. Estimation of US SARS-CoV-2 infections, symptomatic infections, hospitalizations, and deaths using seroprevalence surveys. JAMA Network Open. 2021;4(1):e2033706–e2033706.

52. Mwananyanda L, Gill CJ, MacLeod W, Kwenda G, Pieciak R, Mupila Z, et al. Covid-19 deaths in Africa: prospective systematic postmortem surveillance study. British Medical Journal. 2021;372.

53. Fraser C. Estimating individual and household reproduction numbers in an emerging epidemic. PloS One. 2007;2(8). doi:10.1371/journal.pone.0000758.

54. Gu Y. COVID-19 projections using machine learning.; 2021. https://covid19-projections.com.

55. Situation updates on COVID-19; 2021. https://www.ecdc.europa.eu/en/covid-19/situation-updates.

56. FitzJohn R, Ashton R, Hill A, Eden M, Hinsley W, Russell E, et al.. orderly: Lightweight Reproducible Reporting; 2021. Available from: https://github.com/vimc/orderly.

Figures

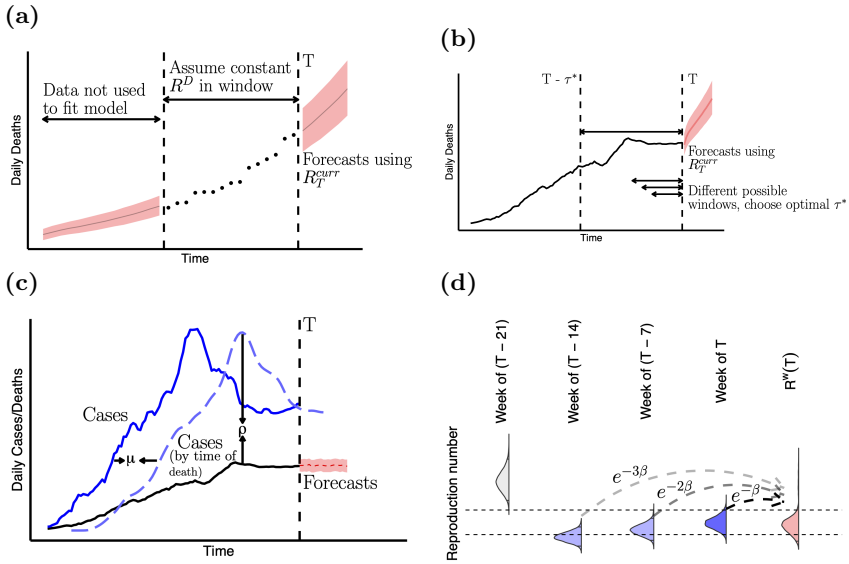

Fig 1. Schematic of the models (a) Model 1 assumes a single value for $R[T-\tau+1,T]$. The model is fitted using only the data in this window ($T-\tau+1$ to T) to jointly estimate the initial incidence of deaths and $R[T-\tau+1,T]$. For details, see SI Sec. 2.1. (b) Model 2 optimises the window over which R_t is assumed to be constant by minimising the cumulative predictive error over the entire epidemic time series. Estimates from $R[T-\tau^*+1,T]$ are used to forecast into the future, with τ^* the window of optimal length. See also SI Sec. 2.2. (c) Model 3 uses data from both cases and deaths (SI Sec. 2.3). The dashed blue curve represents the incidence of reported cases weighted by the case-report to death delay distribution, where μ is the mean delay. ρ_t is the ratio of the observed deaths and the weighted cases at time t and is analogous to an observed case fatality ratio. Forecasts of deaths are obtained by sampling from a binomial distribution using the most recent estimate of ρ_T. See also SI2 Fig. 3. (d) To obtain medium-term forecasts, we combine the most recent transmissibility estimate R_T^{curr} (shown in dark blue) with estimates of transmissibility in the previous weeks to produce a weighted estimate of transmissibility R_T^w (filled in pink) at time T. Estimates from previous weeks are combined with the most recent estimates if the 95% CrI of estimates in week k, R_{T-7k}^{curr} overlaps the 95% CrI of R_T^{curr}. Estimates for weeks where the 95% CrI overlap are shown in light purple, and where the 95% CrI do not overlap in grey. The dashed horizontal lines represent the 2.5th and 97.5th quantile of R_T^{curr}. We combine the estimates by sampling from the posterior distribution of R_{T-7k}^{curr} with probability proportional to $e^{-\beta*k}$, where β is a rate at which the probability decays as we go back in time.

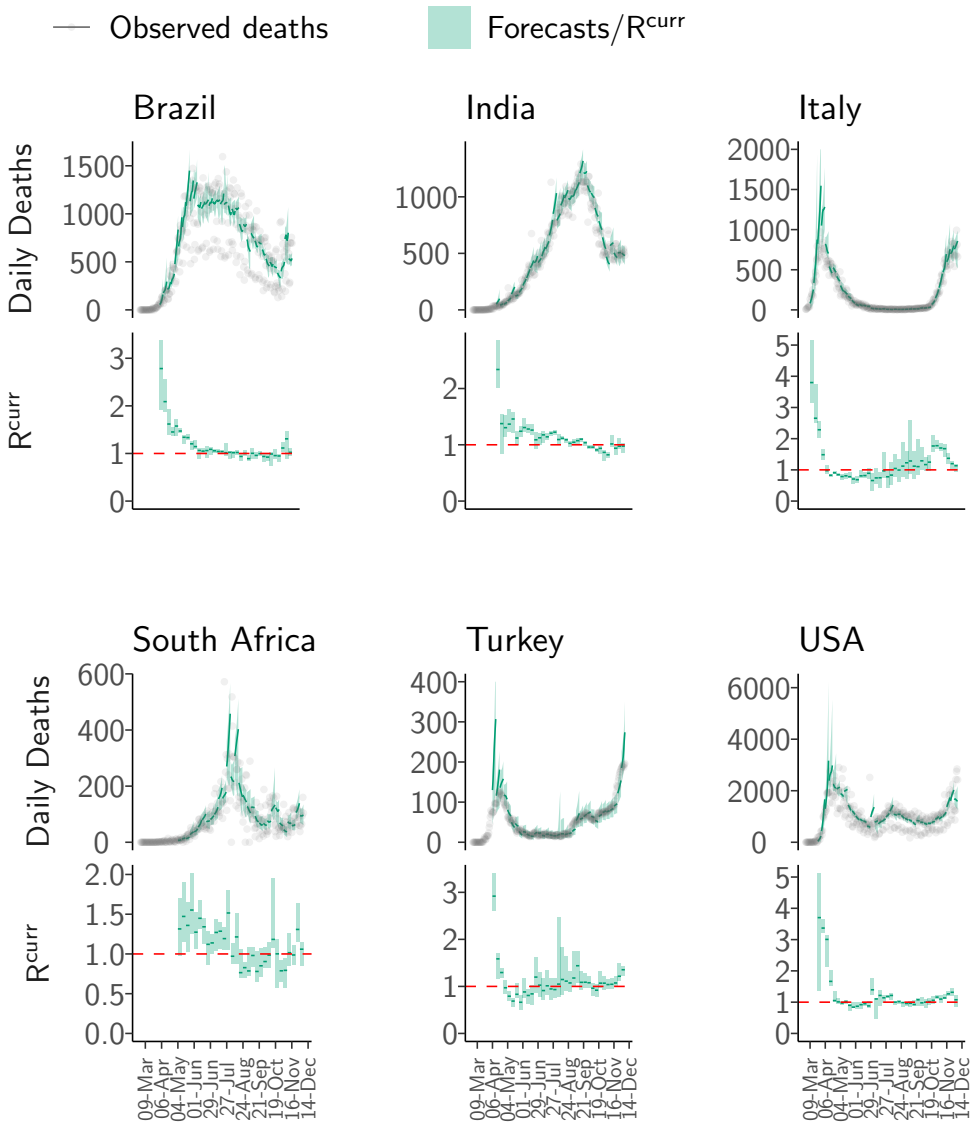

Fig 2. Short-term forecasts. The short-term forecasts and observed deaths for six countries: Brazil, India, Italy, South Africa, Turkey and the United States of America (USA). For each country, the top panel shows the observed deaths in gray; the solid green line shows the median forecast. The shaded interval represents the 95% CrI of forecasts. The forecasts were produced using the most recent estimates of R_T^{curr} assuming that the transmissibility remains constant. The bottom panel for each country shows the effective reproduction number (R_T^{curr}) used to produce the forecasts. The solid green line in the bottom panel for each country is the median estimate of R_T^{curr} while the shaded region represents the 95% CrI. The dashed red line indicates the $R_T^{curr} = 1$ threshold. Note that the y-axis is different for each subfigure. See SI 3 for results for all other countries.

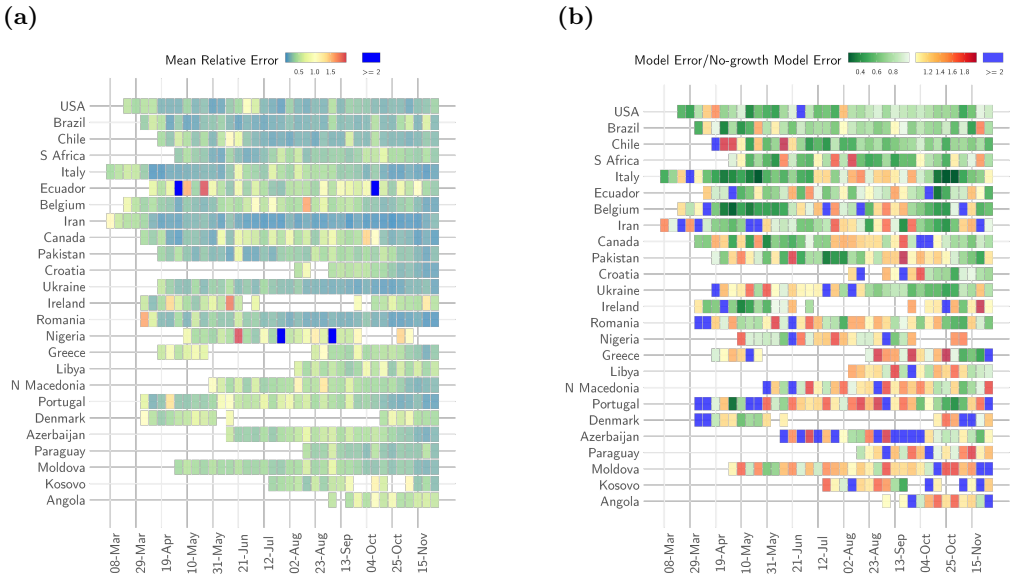

Fig 3. Short-term forecasts MRE and comparison with null model (a) The mean relative error of the ensemble model for each week of forecast (x-axis) and for each country (y-axis). Dark blue cells indicate weeks where the relative error of the model was greater than 2. (b) The ratio of the absolute error of the model to the absolute error of a no-growth null model that uses the average of the last 10 days as a forecast for the week ahead. Shades of green show weeks for a given country where the ratio was smaller than 1 i.e., the ensemble model error was smaller, and weeks where the ratio was greater than 1 i.e. the ensemble model error was larger than the null model error are shown in shades of red (yellow to red). Dark blue indicates weeks when the ratio was larger than 2. In order to present a representative sample, we first ranked all countries by the percentage of weeks in which ensemble model error was smaller than the null model error. We then selected every third country from the top 75 countries in this list. Results for the selected 25 countries are shown here. See SI2 Fig. 1 for the results for other countries. Ordering of countries in the figure reflects the order in the ranked list i.e. countries with the highest percentage of weeks with model error smaller than null model error are shown on the top.

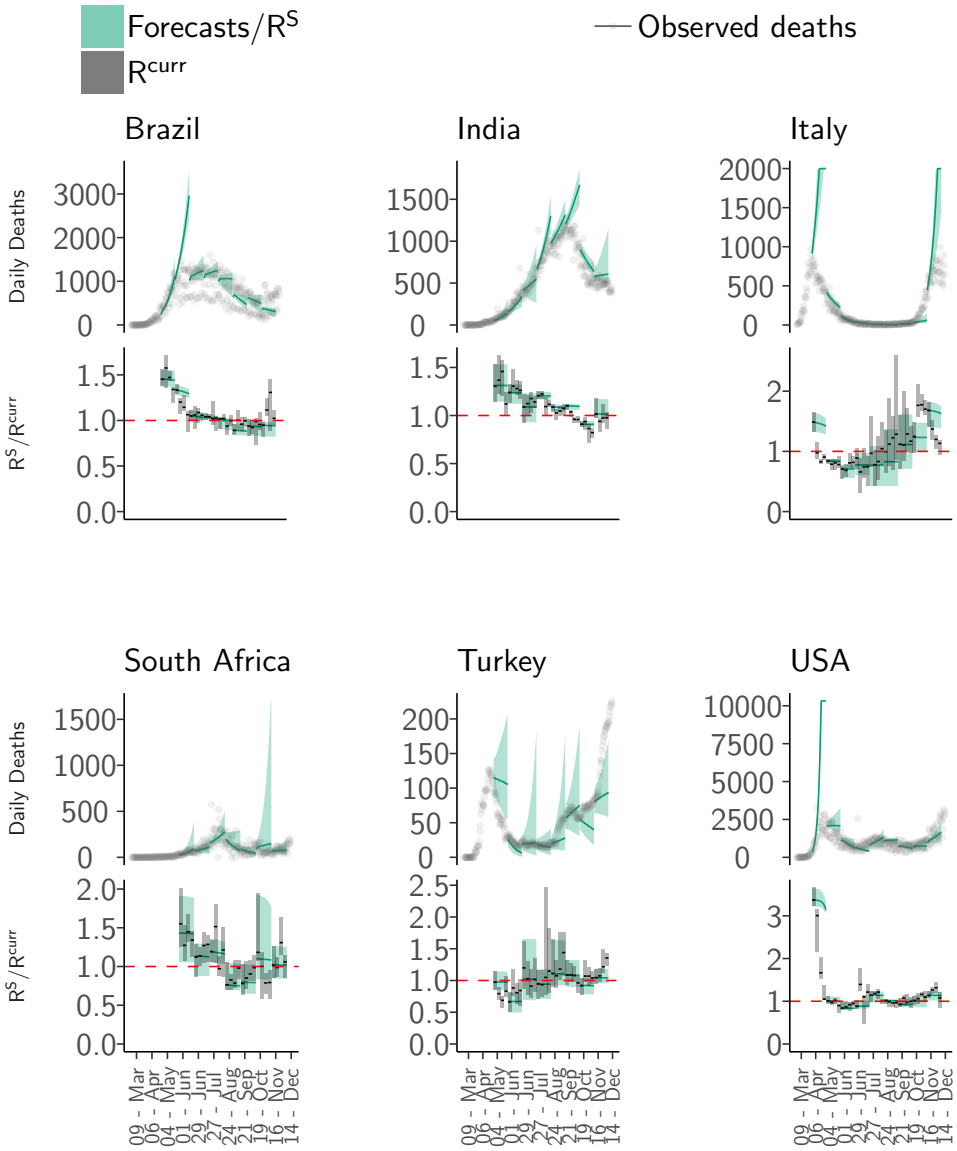

Fig 4. Medium-term forecasts. The medium-term forecasts and observed deaths for six countries: Brazil, India, Italy, South Africa, Turkey and the United States of America (USA). For each country, the top panel shows the observed deaths in grey; the solid green line shows the median the 4-weeks ahead forecast. The shaded interval represents the 95% CrI of forecasts. The bottom panel for each country shows the median (solid black line) and the 95% CrI (grey shaded area) of weekly estimate of R_t^{curr} from the short-term forecasts and the median (green line) and the 95% CrI (shaded green area) of R_t^S i.e. the reproduction number accounting for depletion of susceptible population from the medium-term forecasts over a 4-week horizon (Methods). The dashed red line indicates the $R_t^S = 1$ threshold. Note that the y-axis is different for each subfigure. The forecasts were produced every week over a 4-week forecast horizon. The figure shows all non-overlapping forecasts over the course of the pandemic. See SI 3 for results for all other countries and weeks.

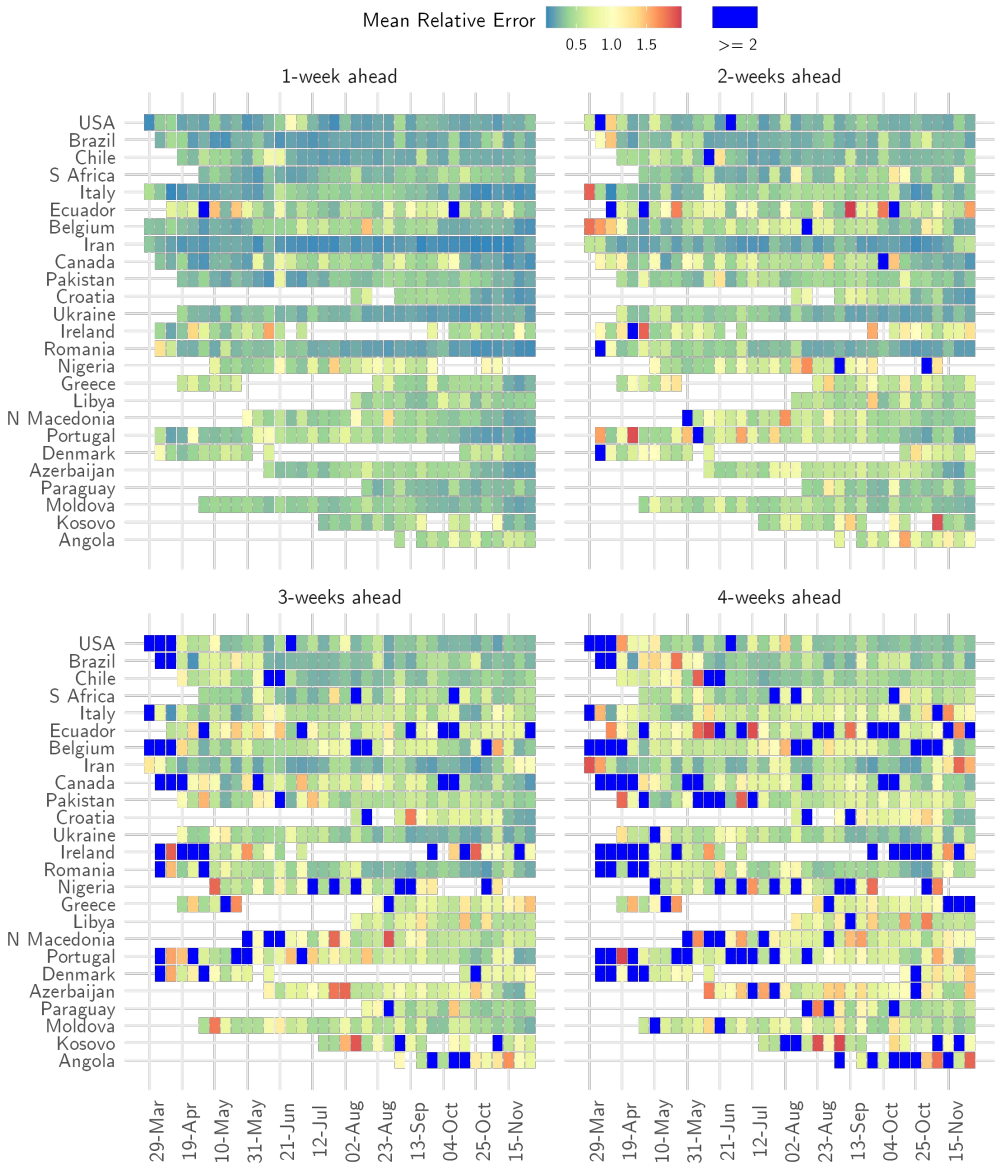

Fig 5. Relative error of medium-term forecasts. The mean relative error of the model in 1-week, 2-week, 3-week and 4-week ahead forecasts for each week when a forecast was made (x-axis) and for each country (y-axis). Blue cells indicate weeks where the relative error of the model was greater than 2. For ease of presentation, results are shown for the same 25 countries as Fig. 2. See SI2 Sec. 2 for the results for other countries.

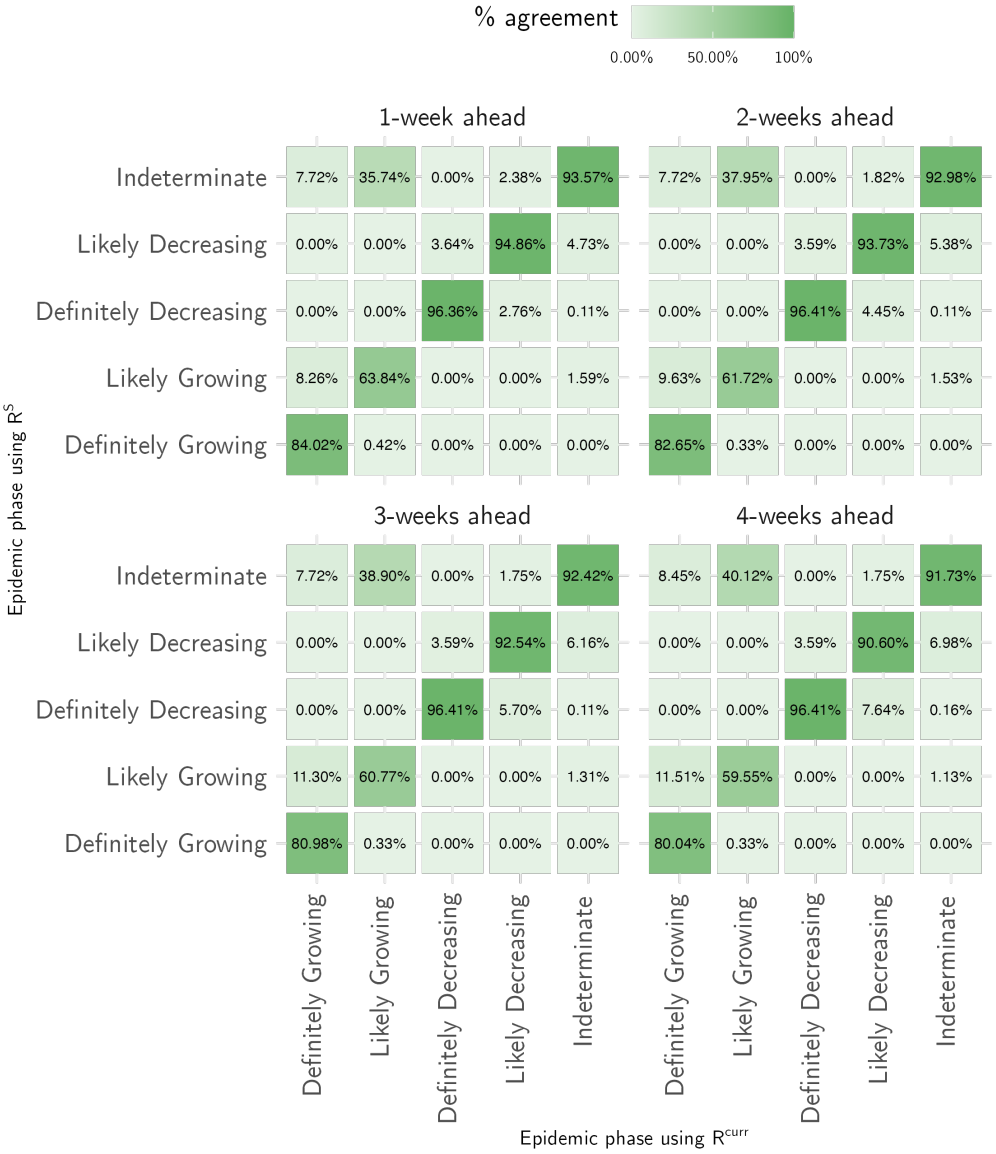

Fig 6. Characterisation of the epidemic phase. For a given classification of epidemic phase using the weekly estimates of the reproduction number from the short-term forecasts(x-axis), the figures in the cell show the percentage of days for which the characterisation was consistent using the medium-term reproduction number estimates (show on the y-axis)

Supplementary Files

This is a list of supplementary files associated with this preprint. Click to download.

- globalforecastsSI1.pdf
- globalforecastsSI2.pdf
- globalforecastsSI1.pdf
- globalforecastsSI2.pdf
- nrsoftwarepolicy.pdf
- nrreportingsummary.pdf